

# We are IntechOpen, the world's leading publisher of Open Access books Built by scientists, for scientists

4,800

Open access books available

122,000

International authors and editors

135M

Downloads

Our authors are among the

154

Countries delivered to

TOP 1%

most cited scientists

12.2%

Contributors from top 500 universities



WEB OF SCIENCE™

Selection of our books indexed in the Book Citation Index  
in Web of Science™ Core Collection (BKCI)

Interested in publishing with us?  
Contact [book.department@intechopen.com](mailto:book.department@intechopen.com)

Numbers displayed above are based on latest data collected.  
For more information visit [www.intechopen.com](http://www.intechopen.com)



# Hybrid Two-step Preparation of Nanosized MgAl Layered Double Hydroxides for CO<sub>2</sub> Adsorption

*Xiani Huang, Xiaogang Yang, Guang Li, Collins I. Ezeh, Chenggong Sun and Collins Snape*

## Abstract

Hybrid Two-step synthesis method for preparation of MgAl LDHs materials for CO<sub>2</sub> adsorption has been employed because of the features of fast micromixing and enhanced mass transfer by using a ‘T-mixer’ reactor. MgAl LDHs with different morphologies were successfully obtained by three different synthesis routes: ultrasonication-intensified in ‘T-mixer’ (TU-LDHs), conventional co-precipitation (CC-LDHs) and ultrasonic-intensified in ‘T-mixer’ pretreatment followed by conventional co-precipitation (TUC-LDHs). The synthesized samples characterized by the XRD showed that LDHs formed a typical layered double hydroxide structure and no other impurities were identified in the compound. The SEM and TEM analyses also confirmed that the size distribution of TUC-LDHs was relatively uniform (with an average size of approximate 100 nm) and layered structure was clearly visible. The BET characterization indicated that such LDHs had a large surface area (235 m<sup>2</sup> g<sup>-1</sup>), which makes it a promising adsorbent material for CO<sub>2</sub> capture in practical application. It can be found that the CO<sub>2</sub> adsorption capacities of TU-LDHs, CC-LDHs and TUC-LDHs at 80°C were 0.30, 0.22 and 0.28 mmol g<sup>-1</sup>, respectively. The CO<sub>2</sub> adsorption capacities of TU-LDHs, CC-LDHs and TUC-LDHs at 200°C were 0.33, 0.25 and 0.36 mmol g<sup>-1</sup>, respectively. The order of CO<sub>2</sub> adsorption capacity to reach equilibrium at 80°C seen in Avrami model is: TU-LDHs > TUC-LDHs > CC-LDHs. The CO<sub>2</sub> adsorption/desorption cycling test reveals that TU-LDHs and TUC-LDHs have good adsorption stability than CC-LDHs.

**Keywords:** MgAl LDHs, ultrasonic, co-precipitation, T-mixer, CO<sub>2</sub> adsorption capacity, Avrami model

## 1. Introduction

The removal of CO<sub>2</sub> emission from fossil fuel combustion, especially from coal-fired power stations, has attracted much attention in recent years because of its potential negative impact on global warming and on human beings. It was reported that CO<sub>2</sub> concentration in atmosphere now is close to 400 ppm, which is significantly higher than the reported industrial level of 300 ppm [1]. CO<sub>2</sub> capture and storage (CCS) technology is considered to be an effective means to cope with the global demand of CO<sub>2</sub> reduction in the long run. Among many technologies existing for CO<sub>2</sub> capture, the use of amine-based solutions is still the main practical

technology on a large scale capture operation which could produce a series of bad effects such as toxicity, degradability, high regeneration energy requirements and corrosivity [2]. Hence, developing efficient and environmental friendly CO<sub>2</sub> adsorbents will be crucial to CO<sub>2</sub> capture. Layered double hydroxides (LDHs) are considered as good candidates for CO<sub>2</sub> adsorption because of their fast sorption/desorption kinetics and simple regenerability [3, 4]. LDHs are a class of ionic lamellar compounds made up of positively charged brucite-like layers with an interlayer region containing charge compensating anions and solvation molecules. The typical structure of LDHs consists of positively charged brucite-like layers, containing anions and water molecules in the interlayer spaces. Metal cations occupy the centre of octahedral structures and hydroxides occupy the vertices. The general formula of LDHs can be expressed as  $[M^{2+}_{1-x}M^{3+}_x(OH)_2][A^{n-}]_{x/n}zH_2O$ , where M<sup>2+</sup> are divalent cations, such as Mg<sup>2+</sup>, Zn<sup>2+</sup>, Ni<sup>2+</sup>, etc., and M<sup>3+</sup> are trivalent cations, such as Al<sup>3+</sup>, Ga<sup>3+</sup>, Fe<sup>3+</sup>, Mn<sup>3+</sup>, etc. A<sup>n-</sup> is a non-framework charge compensating anion, such as CO<sub>3</sub><sup>2-</sup>, Cl<sup>-</sup>, SO<sub>4</sub><sup>2-</sup>, etc., and the value of x is between 0.10 and 0.33 [5].

The performance of LDHs and derived CO<sub>2</sub> adsorbents have been investigated for several years, and most of the studies are focused on the effects of divalent cations [6, 7], trivalent cations [8], charge compensating anions [9, 10], Mg-Al ratio [6, 11, 12], alkaline metal cations (e.g. K<sup>+</sup>, Cs<sup>+</sup>, Na<sup>+</sup>, etc.) [13–16], synthetic method [17], the presence of SO<sub>2</sub> and H<sub>2</sub>O [18, 19], particle size [3, 20] and calcination temperature or adsorption temperature [21, 22]. Yong and Rodrigues compared several commercial hydrotalcite-like compounds that can have the average CO<sub>2</sub> adsorption capacity (0.2–0.5 mmol g<sup>-1</sup>) at 300°C and 1 bar of CO<sub>2</sub> [6]. Wang et al. found that similar CO<sub>2</sub> capture capacities (0.41–0.46 mmol g<sup>-1</sup>) can be obtained when using Mg<sub>3</sub>Al<sub>1</sub>, Mg<sub>3</sub>Ga<sub>1</sub> and Mg<sub>3</sub>Fe<sub>1</sub> at different calcination temperatures [8]. Except for changing the composition of LDHs, controlling its particle size is also believed to be an effective way for improvement of the CO<sub>2</sub> capture capacity. Significant amount of efforts have been made on developing new methods to control its particle size. Hanif et al. investigated the effect of synthetic routes (co-precipitation, ultrasonication and microwave irradiation) on improving the CO<sub>2</sub> adsorption capacity of hydrotalcite-based sorbents in the temperature range 300–400°C [17]. They have reported that the CO<sub>2</sub> adsorption capacity of LDHs prepared by ultrasound-assisted route and microwaving are better than that of co-precipitation method.

Adoption of confined impinging T-jet mixer (CITJ) is a simple component that contains two inlet tubes and let two streams flow out from the tube. The local micromixing effect could be intensified during the CITJ reactor, which is beneficial for a fast homogenization of reactors. The mass transfer rate and chemical reaction rate can also be enhanced during the preparation process. This has been confirmed by the studies on the preparation of FePO<sub>4</sub> nanoprecursor particles of LiFePO<sub>4</sub> cathode material where the high specific areas can be obtained [23, 24]. Co-precipitation method is the conventional procedure used for synthesis of hydrotalcites. Ultrasonication and microwave irradiation of the synthesis gel during hydrotalcite precipitation leads to disruption in the layer stacking which in turn increases surface area [17]. To the best of our knowledge, the effect of the synthesis for the preparation of LDHs by applying jointly co-precipitation and ultrasonication in a T-jet mixer on the CO<sub>2</sub> absorption capacity of LDHs has not yet been reported in the literature.

In the present study, we will present a hybrid two-step method approach for preparation of MgAl layered double hydroxide (MgAl LDHs). The novel two-step preparation route utilising the MgAl LDHs synthesized from confined impinging T-jet mixer (CITJ) as seeds for future preparation. The synthesized samples were

characterized using X-ray diffraction (XRD), scanning electron microscopy (SEM), transmission electron microscopy (TEM) and BET analysis. Their performance of CO<sub>2</sub> adsorption was evaluated using thermogravimetric analysis (TGA). The effect of the rate of addition of Mg(NO<sub>3</sub>)<sub>2</sub> and Al(NO<sub>3</sub>)<sub>3</sub> on improvement of the CO<sub>2</sub> capture capacity of MgAl LDHs and initial NH<sub>3</sub>H<sub>2</sub>O is also investigated.

## 2. Experimental

### 2.1 Materials preparation

#### 2.1.1 LDH synthesized in T-Mixer with ultrasonic process

Salt solution A (100 mL) containing a mixture of 0.03 mol L<sup>-1</sup> Mg(NO<sub>3</sub>)<sub>2</sub> and 0.01 mol L<sup>-1</sup> Al(NO<sub>3</sub>)<sub>3</sub> and solution B-NH<sub>3</sub>H<sub>2</sub>O (100 mL) with certain concentration was simultaneously transported into a 'T-type' impinging-stream reactor by means of metering pumps at the rate of 100 r min<sup>-1</sup> to produce MgAl LDHs. Ultrasonic processing was also applied during this process and the frequency of ultrasonic processing kept to be 20 kHz. The pH of the whole solution was always kept to be 10 ± 0.2 though regulating the concentration of NH<sub>3</sub>H<sub>2</sub>O. The resulting mixture washed with water for several times until pH = 7 and then dried at 100°C in an oven. The resulting material was denoted as **TU-LDHs**.

#### 2.1.2 LDH synthesized by conventional co-precipitation method

For the synthesis of traditional LDHs, LDHs was prepared by co-precipitation method. The salt solution with a fixed concentration of 0.03 mol L<sup>-1</sup> Mg(NO<sub>3</sub>)<sub>2</sub> and 0.01 mol L<sup>-1</sup> Al(NO<sub>3</sub>)<sub>3</sub>-A (200 mL) with a certain rate of addition and 1 mol L<sup>-1</sup> of NH<sub>3</sub>H<sub>2</sub>O were simultaneously added to the mixture at the second step, where the pH of the whole solution was always kept to be 10 ± 0.2 and continuous stirring rate is 400 r min<sup>-1</sup>. The mixture was then aged for further 4 h with stirring maintained. The final obtained materials were filtered and washed with distilled water until pH = 7, followed by drying at 100°C in an oven. The obtained material was denoted as **CC-LDHs**.

#### 2.1.3 LDH synthesized by hybrid two-step method

MgAl layered double hydroxides (MgAl LDHs) were prepared using a hybrid two-step preparation approach. The hybrid two-step preparation consists of the mother solution prepared in 'T-mixer' accompanying with ultrasonic processing (first step) and the following step of co-precipitation (second step) process. The mother solution was synthesized according to the preparation method of the above section. About 50 mL of mother solution from the above solution was put into a beaker for continuous stirring with a rate of 400 r min<sup>-1</sup>. Then, 150 mL of salt solution with a fixed concentration of 0.03 mol L<sup>-1</sup> Mg(NO<sub>3</sub>)<sub>2</sub> and 0.01 mol L<sup>-1</sup> Al(NO<sub>3</sub>)<sub>3</sub> and 1 mol L<sup>-1</sup> of NH<sub>3</sub>H<sub>2</sub>O were simultaneously added to the mixture at the second step. The addition rate of salt solution was controlled by regulating the speed of peristaltic pump, where the pH of the whole solution was always kept to be 10 ± 0.2. The whole preparation process of MgAl LDHs by two steps were illustrated in **Figure 1**. The final obtained materials were filtered and washed with distilled water until pH = 7, followed by drying at 100°C in an oven. The obtained material was denoted as **TUC-LDHs**.

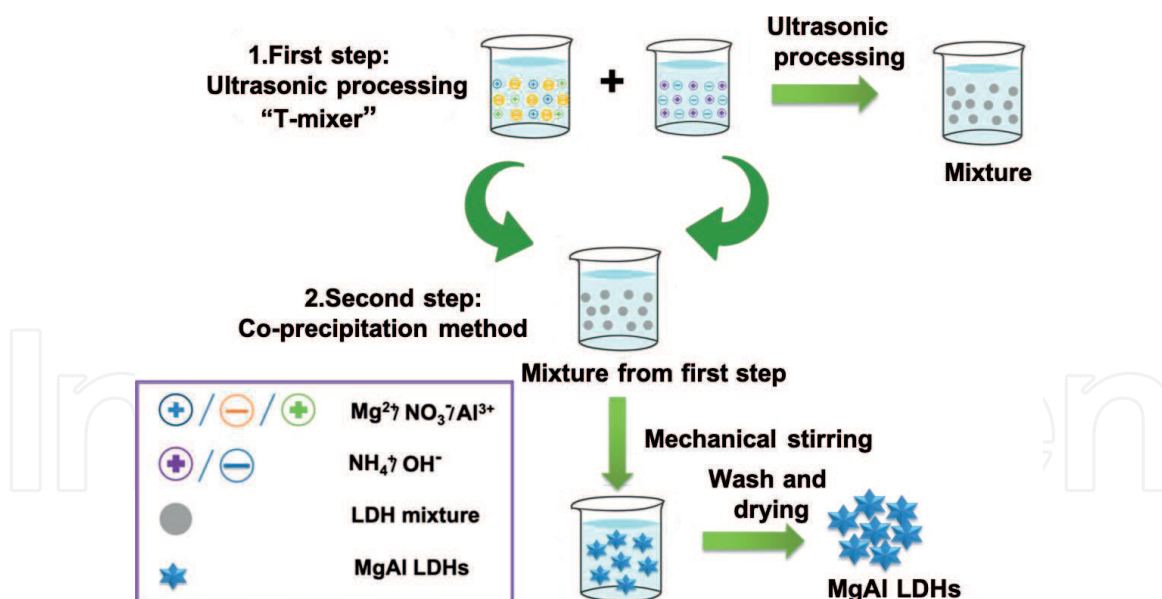


**Figure 1.**  
Schematic illustrating the preparation process of MgAl LDHs by hybrid two steps.

## 2.2 Materials characterization

The structures of MgAl LDHs were characterized using a combination of methods including BET-specific surface areas, X-ray diffraction (XRD), scanning electron microscopy (SEM), energy dispersive X-ray spectroscopy (EDX) analysis and transmission electron microscope (TEM).

### 2.2.1 BET

Nitrogen adsorption/desorption isotherms were carried out on a Micromeritics ASAP2020 surface area and pore size analyser at 77 K. Before conducting each measurement, the prepared LDHs were first degassed at 110°C overnight.

### 2.2.2 XRD

The structure of the prepared samples were analysed by XRD through conducting in a Bruke-AXS D8 advance powder diffractometer using Cu-K $\alpha$  radiation ( $\lambda = 1.5418 \text{ \AA}$ ) and a power of 40 kv\*20 Ma, where the diffraction patterns were recorded in the range  $2\theta = 5\text{--}80^\circ$  with a step size of  $0.01^\circ$ .

### 2.2.3 SEM and EDXS

The morphologies of synthesized LDHs were observed using SEM produced from ZEISS ZIGMA 174C CZ. The element analysis was conducted by use of an Oxford Instrument INCAx-act PentaFET® Precision EDXs.

### 2.2.4 TEM

High-resolution TEM images were obtained using JEM-2100 electron microscope operating at 200 kV, whereby a drop of solution was placed onto a Cu grid and dried in infrared lamp for several minutes.

### 2.3 Carbon dioxide adsorption measurements

The CO<sub>2</sub> adsorption test and regenerability of the synthesized adsorbents were measured by Netzsch TG 209 F1 thermogravimetric analyser (TGA) at atmosphere pressure under dry conditions. Pure CO<sub>2</sub> gas was used to carry out the whole adsorption/desorption measurement. Before adsorption test, all the samples were calcined at 500°C for 5 h in an Ar atmosphere. About 10 mg of sample loaded into an alumina crucible was heated from 25 to 105°C at 10°C min<sup>-1</sup> under N<sub>2</sub> atmosphere for 60 min and then switched to desired temperature (80, 150 and 200°C) at the rate of 10°C min<sup>-1</sup>. During the isothermal stage, the gas input changed from N<sub>2</sub> to CO<sub>2</sub> and held for 90 min. The CO<sub>2</sub> adsorption capacity of the sample- $q_t$  (mmol g<sup>-1</sup>) was calculated according to the weight gain of the sample and expressed as the mole of CO<sub>2</sub> absorbed per gram of adsorbent:

$$q_t = \frac{m_t - m_o}{m \times M} \times 1000 \quad (1)$$

where  $m_o$  and  $m_t$  (mg) are the initial mass of adsorbent for CO<sub>2</sub> adsorption and mass of adsorbent for CO<sub>2</sub> adsorption at time t, respectively.  $m$  is the total mass of sorbent (mg) and  $M$  is molar mass of CO<sub>2</sub> (44 mol g<sup>-1</sup>).

In the absorption/desorption cycle, about 10 mg of the above calcined samples was heated from 25 to 105°C at 10°C min<sup>-1</sup> under N<sub>2</sub> atmosphere (40 mL min<sup>-1</sup>) for 60 min and then switched to 80°C at a cooling rate of 10°C min<sup>-1</sup>. After adsorption, the desorption process was carried out as the gas input was switched from CO<sub>2</sub> to N<sub>2</sub> at 105°C. The adsorption/desorption process was repeated in six cycles.

### 2.4 Error analysis

To determine the validity of isotherm and kinetics models, two different error functions, i.e. chi-square ( $X^2$ ) and normalized standard deviation  $\Delta q$ (%), and correlation coefficient equation  $R^2$  were evaluated between experimental and calculated data, which are given by

$$\text{Chi - square : } X^2 = \sum_{i=1}^n \frac{(q_t - q_e)^2}{q_e} \quad (2)$$

$$\text{Normalized standard deviation : } \Delta q(\%) = \sqrt{\frac{\sum_{i=1}^n [(q_t - q_e)/q_e]^2}{n - 1}} \times 100 \quad (3)$$

$$\text{Correlation coefficient equation : } R^2 = 1 - \left( \frac{\sum_{j=1}^N (q_t - q_e)^2}{\sum_{j=1}^N (q_t - \bar{q}_e)^2} \right) \times \left( \frac{N - 1}{N - p} \right) \quad (4)$$

where  $q_t$  and  $q_e$  are CO<sub>2</sub> uptake determined by experiment and computed by model, respectively.  $q_e$  is the mean experimental data,  $p$  is the number of model parameters and  $N$  is total number of experimental points. The most suitable model to describe the CO<sub>2</sub> adsorption process is the one with highest  $R^2$  value.

### 3. Results and discussion

#### 3.1 Synthesis and characterization of LDHs prepared by different ways

Co-precipitation method is a common method used in preparation of MgAl LDHs materials in the previous studies. The main requirement for improving the CO<sub>2</sub> adsorption capacity of MgAl LDHs is to develop it with high surface area and pore volume. It is well known that the formation process of MgAl LDHs includes both nucleation and growth process. Controlling the process of nucleation properly may have an effect on the whole size of MgAl LDHs, thus increasing its surface area. Here, we reported the first synthesis of MgAl LDHs using a hybrid two-step method. At first step, the salt solution and initial concentration of NH<sub>3</sub>H<sub>2</sub>O solution were transported into ‘T-type’ impinging-stream reactor. Two solutions interact on each other on the ‘T-type’ impinging-stream reactor and ultrasonic wave were also applied in the interaction process. At second step, the conventional co-precipitation method was used. This means that a certain rate of salt solution and NH<sub>3</sub>H<sub>2</sub>O were simultaneously added to the mixture to produce the MgAl LDHs. The chemical and physical effects of ultrasonic irradiation originated from acoustic cavitation lead to rapid reaction rate and change the selectivity performance of the reaction [25], thus improving the nucleation of MgAl LDHs.

The XRD patterns of MgAl LDHs prepared using three different methods are shown in **Figure 2**. For all the samples, the characteristic reflections based on the structure of (PDF #35-0965) were clearly observed, which can be indexed to (i) (00*l*) peaks of (003) and (006) with corresponding to the basal spacing and higher order reflections; (ii) (0*kl*) peaks of (012), (015) and (018) with broad reflections; (iii) sharp (*hk*0) and (*hkl*) peaks of (110) and (113). It can be seen that LDHs samples synthesized under different conditions have similar structures. The lattice parameter *a* and *c* are calculated according to the parameters of (110) and (003) plane assuming a 3R stacking of layer structure, where the value *a* ( $a = 2d_{110}$ ) represents average distance between two metal ions and *c* is three times of the brucite-like layer and interlayer distance ( $d_{003}$ ). The lattice parameter *a* is almost independent of the synthesis method, which can be explained that it was affected

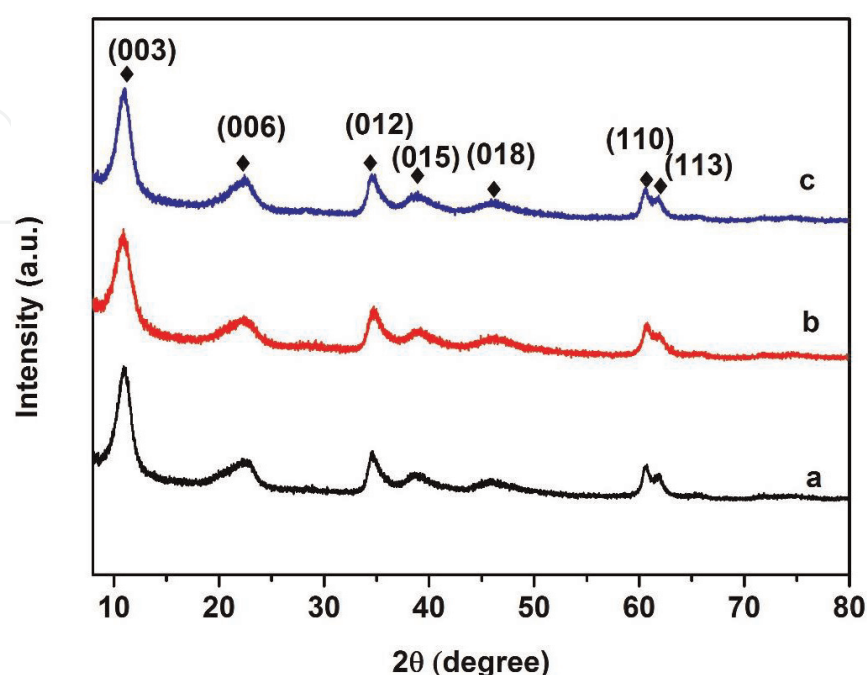


**Figure 2.** XRD patterns for MgAl LDHs prepared using (a) TU method, (b) CC method and (c) TUC method.

by the type of metal cation (Mg<sup>2+</sup> and Al<sup>3+</sup>). Although LDHs are prepared by three different ways, the metal cation of Mg<sup>2+</sup> and Al<sup>3+</sup> still keep the same without any change. Similar observations can be found in the research of Wang et al. for the formation of LDHs by co-precipitation and IEP method [20]. Concerning the lattice parameter c, it was affected by three main factors: the average charge of the metal cations, the nature of the interlayer anion and the water content. TU-LDHs have lowest lattice parameter c compared to other two LDHs. All the samples use the same anion and metal cations so that the slight difference between samples may be related to a slow water content in the layer.

The crystalline size of particles was calculated using the *Debye-Scherrer's formula*

$$D = \frac{0.89\lambda}{\beta \cos \theta} \quad (5)$$

where D is the grain size (nm), λ is the wavelength of the X-ray radiation, β is the full width at half maximum and λ, θ is the angle of diffraction. The crystallite size along the c direction was calculated according to (003) and (006) diffraction peaks. The values given in **Table 1** showed that the crystallite size in the c direction by TU-LDHs and TUC-LDHs were a slightly higher than the crystallite size of CC-LDHs. There is no obvious reduction of crystallite size in the c direction of materials prepared by three different methods.

N<sub>2</sub> adsorption-desorption isotherm of MgAl LDHs is given in **Figure 3**. All the adsorbents show a Type IV isotherm according to the IUPAC classification, which is associated with mesoporous materials [26]. TUC-LDHs and CC-LDHs show a H3 type hysteresis loop, suggesting that the pores are produced by 'slit-shaped' of plate-like particles [27]. This type of isotherm is commonly observed in the mesoporous stacking structure of sheet-like 2D crystallites [28]. In the case of TU-LDHs, it shows a H2 type hysteresis loop corresponding to a complex and interconnected pore structure, indicating that the pores are produced by rapid nucleation process. This difference could be related to the different synthetic route applied in this work. The surface area (S<sub>BET</sub>) of the samples were determined using BET (Brunauer, Emmett and Teller) model. The total volumes (V<sub>Total</sub>) were calculated according to the amount of nitrogen (N<sub>2</sub>) absorbed at a relative pressure (P/P<sub>O</sub>) of 0.99. The pore volumes were calculated from the desorption branch of the isotherms using the Barrett-Joyner-Halenda (BJH) method, for the pores between 1.7 and 300.0 nm. **Table 2** lists the textural parameters of MgAl LDHs obtained from N<sub>2</sub> adsorption-desorption isotherms. It can be seen clearly that the S<sub>BET</sub> of TUC-LDHs is the highest of 235.3 m<sup>2</sup> g<sup>-1</sup> compared to 198.7 m<sup>2</sup> g<sup>-1</sup> for TU-LDHs and 148.1 m<sup>2</sup> g<sup>-1</sup> for CC-LDHs as well as the pore sizes (90.83 Å) and highest pore

Property	TU-LDHs	CC-LDHs	TUC-LDHs
d <sub>003</sub> (nm)	0.7977	0.8058	0.8011
d <sub>110</sub> (nm)	0.1518	0.1516	0.1519
a <sup>a</sup> (nm)	0.3036	0.3032	0.3038
c <sup>b</sup> (nm)	2.3931	2.4174	2.4033
Crystallite size in c direction (nm) <sup>c</sup>	8.65	7.35	8.63

$$^a a = 2d_{110}$$

$$^b c = 3d_{003}$$

<sup>c</sup>Value calculated from (003) and (006), according to Debye-Scherrer's formula.

**Table 1.**  
 Lattice parameters of LDHs prepared by different methods.



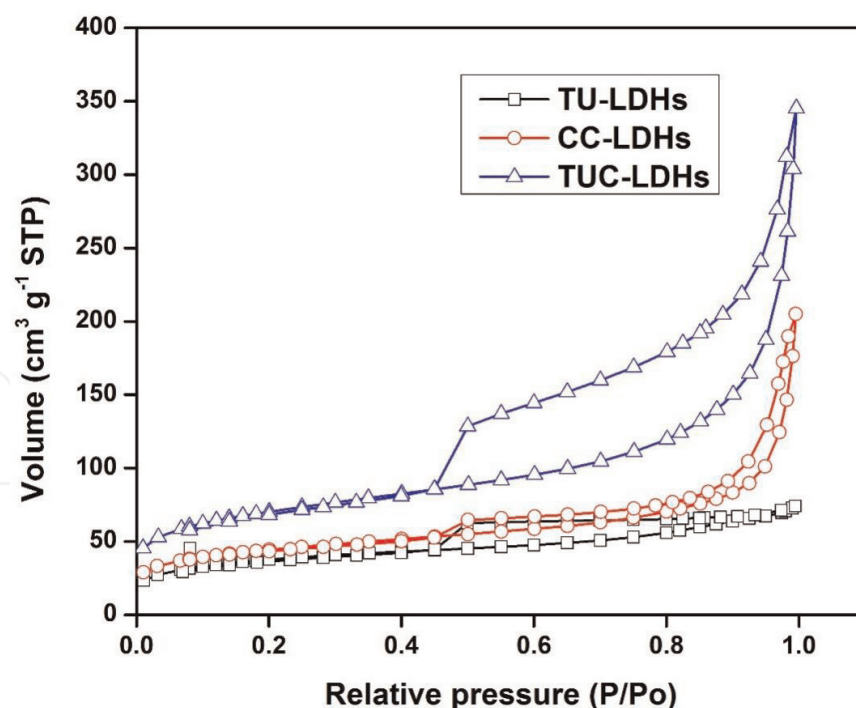


**Figure 3.**  
Nitrogen adsorption-desorption isotherm for TU-LDHs, CC-LDHs and TUC-LDHs.

Sample name	BET surface area ( $\text{m}^2 \text{g}^{-1}$ )	Average pore diameter ( $\text{\AA}$ )	Pore volume ( $\text{cm}^3 \text{g}^{-1}$ )
TU-LDHs	198.7	24.4	0.08
CC-LDHs	148.1	85.61	0.28
TUC-LDHs	235.3	90.83	0.48

**Table 2.**  
Textural parameters of MgAl LDHs obtained from  $\text{N}_2$  adsorption-desorption isotherms.

volume ( $0.48 \text{ cm}^3 \text{g}^{-1}$ ). Both of TUC-LDHs and CC-LDHs facilitate the macro-structure of pores. Although TU-LDHs has the second largest  $S_{\text{BET}}$ , its pore sizes ( $24.4 \text{ \AA}$ ) and pore volume ( $0.08 \text{ cm}^3 \text{g}^{-1}$ ) are the lowest in comparison with other two materials. This indicates that the TU method contributes to the formation of mesoporous structure. The increase in surface area of TU-LDHs is very likely caused by the enhanced micromixing in the ‘T-mixer’, where the use of ultrasonication can intensify the turbulent eddies and those microbubble bursting that erode the surface area of hydrotalcites of layered structure through removal of the interlayer anions [17]. This effect may be more evident as TUC-LDHs compared with CC-LDHs possess smaller size so that the erosion can be taking place for TUC-LDHs. This explanation seems to be supported by SEM and TEM observation of TUC-LDHs.

The size, morphologies and structure of MgAl LDHs prepared by different methods are characterized using FESEM. It can be clearly seen from **Figure 4(a)** that the morphology and structure of TU-LDHs looks like a house-of-cards-type stacking structure, which is similar to that from ‘exfoliation-self-assembly’ method. However, no significant differences can be observed between CC-LDHs and TUC-LDHs, as shown in **Figure 4(b)** and **(c)**. Both of them show rose-like morphology, while morphology of TUC-LDHs looks quite loose compared with CC-LDHs. In order to further explore the morphology and structure of the prepared LDHs, CC-LDHs and TUC-LDHs were also characterized using TEM analysis. The TEM image in **Figure 4(f)** shows that the TUC-LDHs has an average size of 100 nm and

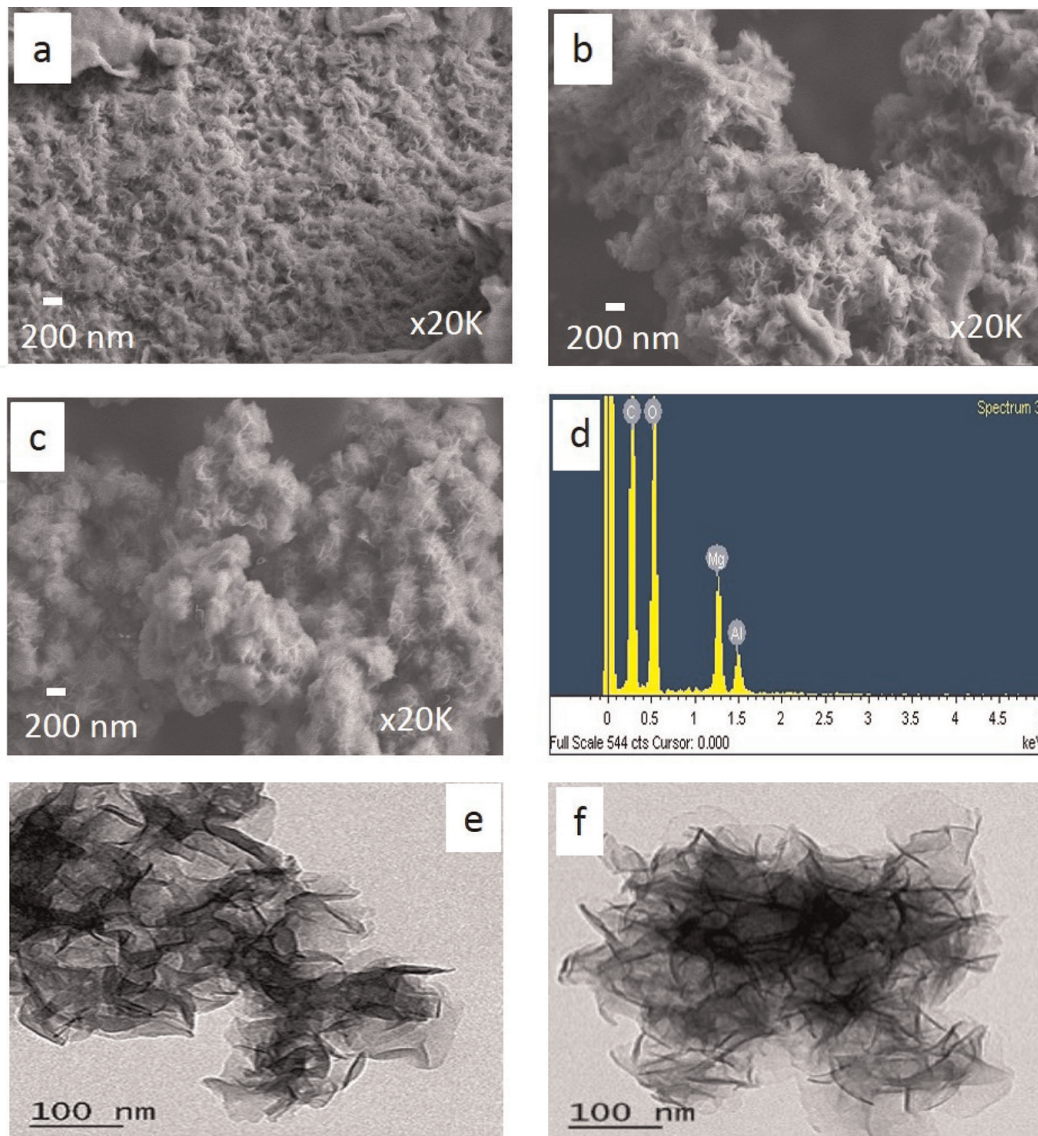


**Figure 4.** SEM images of MgAl LDHs for (a) TU-LDHs, (b) CC-LDHs and (c) TUC-LDHs; EDS of (d) TUC-LDHs; TEM of (e) CC-LDHs and (f) TUC-LDHs.

thickness of 10–20 nm. However, the average size and thickness of CC-LDHs (shown in **Figure 4(e)**) are significantly larger than in the case of TUC-LDHs. In addition, EDX analysis of TUC-LDHs (shown in **Figure 4(d)**) is given as a rough molar ratio of  $M_{\text{Mg}/\text{Al}} \approx 3$ , which is consistent with chemical composition of raw materials.

From the above XRD, BET, SEM and TEM results, further analyses are as follows. Mixing is very slow, relying on the molecular diffusion process due to the absence of turbulence in a low Reynold number. However, the mixing can be enhanced by changing the geometry of mixing channel from conventional agitated vessel to ‘T-mixer’. Ultrasonic wave, an external energy force, can generate additional force to interfere with the flow field in the ‘T-mixer’ channel so that a high level of supersaturation is generated and micromixing process of chemical reaction can be enhanced in extremely short time ( $\sim 10^{-7}$  s) [23, 24]. Thus, the high level of supersaturation contributes to form large amounts of nuclei in a short time, resulting in a small average particle size accumulating together, which is consistent with the BET results in **Table 2**. Finally, the layered structure of TU-LDHs seems to stack together tightly. For TUC-LDHs, the presence of TU-LDHs during the growth of TUC-LDH may introduce defects into LDH structure, through modified nucleation conditions or induced curvature [29]. The final particles exhibit fluffy shapes

and the flake-like structures are formed. Another important reason may be related to the isoelectric point (IEP) of MgAl LDHs. The IEP of MgAl LDHs is around 10, so it can be positively ( $\text{pH} > \text{IEP}$ ), neutrally ( $\text{pH} = \text{IEP}$ ), or negatively ( $\text{pH} < \text{IEP}$ ) charged depending on the relationship between the IEP and the pH. Because it is electronic neutrally on its surface, its growth is inhibited due to the repulsive force between negatively charged TUC-LDH primary particles and  $\text{Al}(\text{OH})_4^-$ ,  $\text{CO}_3^{2-}$ ,  $\text{OH}^-$  anions. Hence, the formation rate of LDHs is so fast that the growth in all directions under such basic conditions. It is well known that the formation process of TUC-LDH includes both nucleation and growth process. In our experiment, the growing of TUC-LDH is based on the mixture solution, which suggests that it supplies a nucleation environment for TUC-LDH growth, then the directions of LDHs growth could be determined. As reported in literature, the deposition of a colloidal suspension of TUC-LDH on substrates, such as glass or silicon, generally leads to the TUC-LDH nanoplatelets having preferred orientation with their c-axis perpendicular to the substrate. The fact that the MgAl- $\text{CO}_3$  LDH nanoplatelets are perpendicularly attached to the surface via their edges suggests they are grown onto the substrate via a strong chemical interaction. Wang et al. reported the first synthesis of nanosized spherical MgAl LDHs using IEP method [20].

### 3.2 TGA analysis

Calcination is a very important step for activating the MgAl LDHs, because the fresh LDHs do not contain much basic sites so that the  $\text{CO}_2$  uptake capacity is quite low. **Figure 5** shows the TGA spectrum of the three different types of synthesized LDHs. The curves for the LDHs prepared by three methods are all fairly similar in shape. The TGA spectra of TU-LDHs show a weight loss of 13% between 50 and 207°C due to the loss of the physisorbed water. In the second weight loss, 33.2% occurred between 207 and 600°C, which is mainly caused by dehydroxylates and decarbonates of LDHs to a large extent, finally leading to the formation of a mixed oxide with a three-dimensional network [8]. For CC-LDHs, the first weight loss

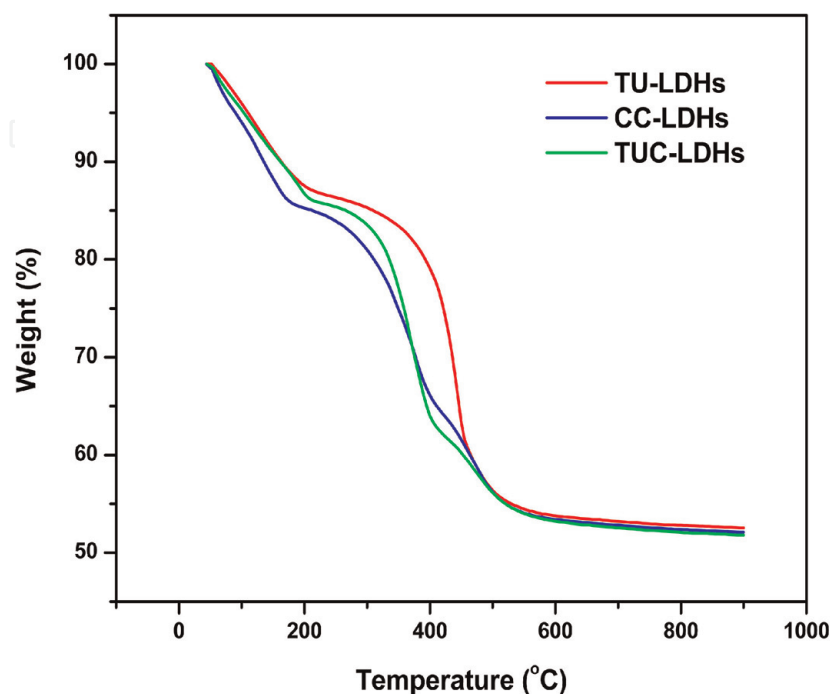


**Figure 5.**  
TGA spectrum of the three different types of synthesized LDHs.

(14%) was found to occur between 50 and 170°C. In the temperature range of 50 and 214°C, TUC-LDHs observed a weight loss of 14%. There are no much differences during the second weight loss process among three samples.

### 3.3 CO<sub>2</sub> adsorption capacity

The CO<sub>2</sub> capture capacity of the above-mentioned three types of LDHs, including TU-LDHs, TUC-LDHs and CC-LDHs, were evaluated using isothermal CO<sub>2</sub> adsorption tests. In the present work, we are particularly interested in whether the modified methods would influence the final CO<sub>2</sub> adsorption capacity or not. The CO<sub>2</sub> adsorption capacities of the different types of LDHs are given in **Figure 6**. All the samples were first calcined at 500°C before each CO<sub>2</sub> adsorption test. Then, the thermogravimetric adsorptions of CO<sub>2</sub> on the samples were measured at 80, 150 and 200°C using a TGA analyser. It can be found that the CO<sub>2</sub> adsorption capacities of TU-LDHs, CC-LDHs and TUC-LDHs at 80°C are 0.30, 0.22 and 0.28 mmol g<sup>-1</sup>, respectively. While for the sample at 200°C, the CO<sub>2</sub> adsorption capacities of TU-LDHs, CC-LDHs and TUC-LDHs are 0.33, 0.25 and 0.36 mmol g<sup>-1</sup>, respectively. The CO<sub>2</sub> adsorption capacity of LDHs at 200°C was higher than that of 80 and 150°C. The main reason maybe that a surface phenomenon and chemical interactions are restricted at 80°C due to the higher activation energy [19]. We can see that TUC-LDHs had better adsorption capacity than other two TU-LDHs and CC-LDHs independent of adsorption temperature. The removal of water during calcination process leads to the formation of channels and pores. As the BET surface area of TUC-LDHs is higher than TU-LDHs and CC-LDHs, it could increase more basic sites for CO<sub>2</sub> adsorption [7].

### 3.4 Kinetic studies of CO<sub>2</sub> capture performance

In order to get a good adsorbent, fast adsorption kinetics is considered as one of the most important parameters to evaluate the adsorbent in a dynamic process. Hence, the ability of withstanding large adsorbate flows are connected with the rate of adsorption. Here, we mainly study the PFO model and Avrami model on the function of CO<sub>2</sub> adsorption on our LDHs [30]. The general sorption rate equations are expressed as:

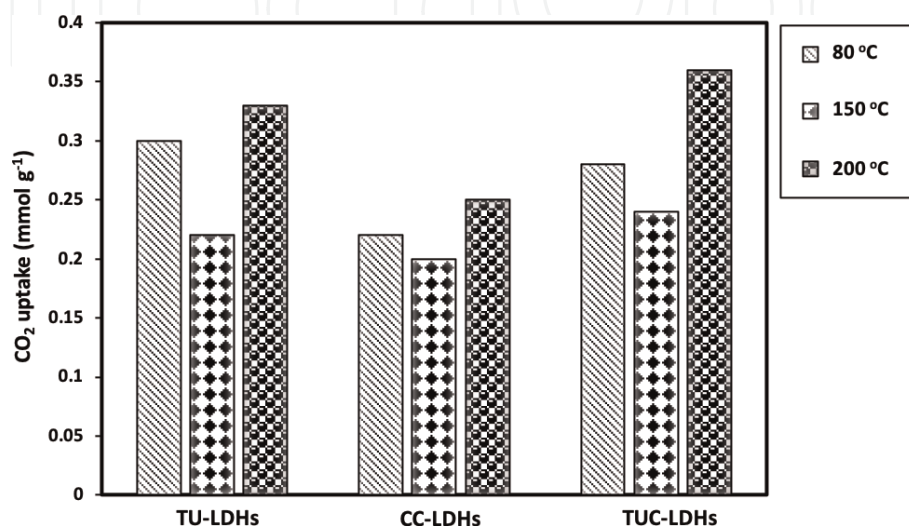


**Figure 6.**  
CO<sub>2</sub> adsorption capacities of the different types of LDHs at different temperatures.

Pseudo-first-order (PFO) model:

$$q_t = q_e(1 - \exp(-k_f t)) \quad (6)$$

Avrami model:

$$q_t = q_e(1 - \exp(-(k_A t)^{n_A})) \quad (7)$$

where  $q_e$  is the adsorption capacity at equilibrium and at time  $t$ , respectively,  $k_f$  is the kinetic parameter of pseudo-first order model,  $k_A$  is the kinetic parameter of Avrami model, the Avrami exponent and  $n_A$  is a fractionary number, which reflects the adsorption mechanism.

To investigate the CO<sub>2</sub> adsorption kinetics of LDHs, **Figure 7** shows that the CO<sub>2</sub> uptake vs. time of TU-LDHs, CC-LDHs and TUC-LDHs at 80, 150 and 200°C and the corresponding profiles as predicted by pseudo-first-order and Avrami kinetic models. From the figure, it could be seen that the adsorption curves of LDHs

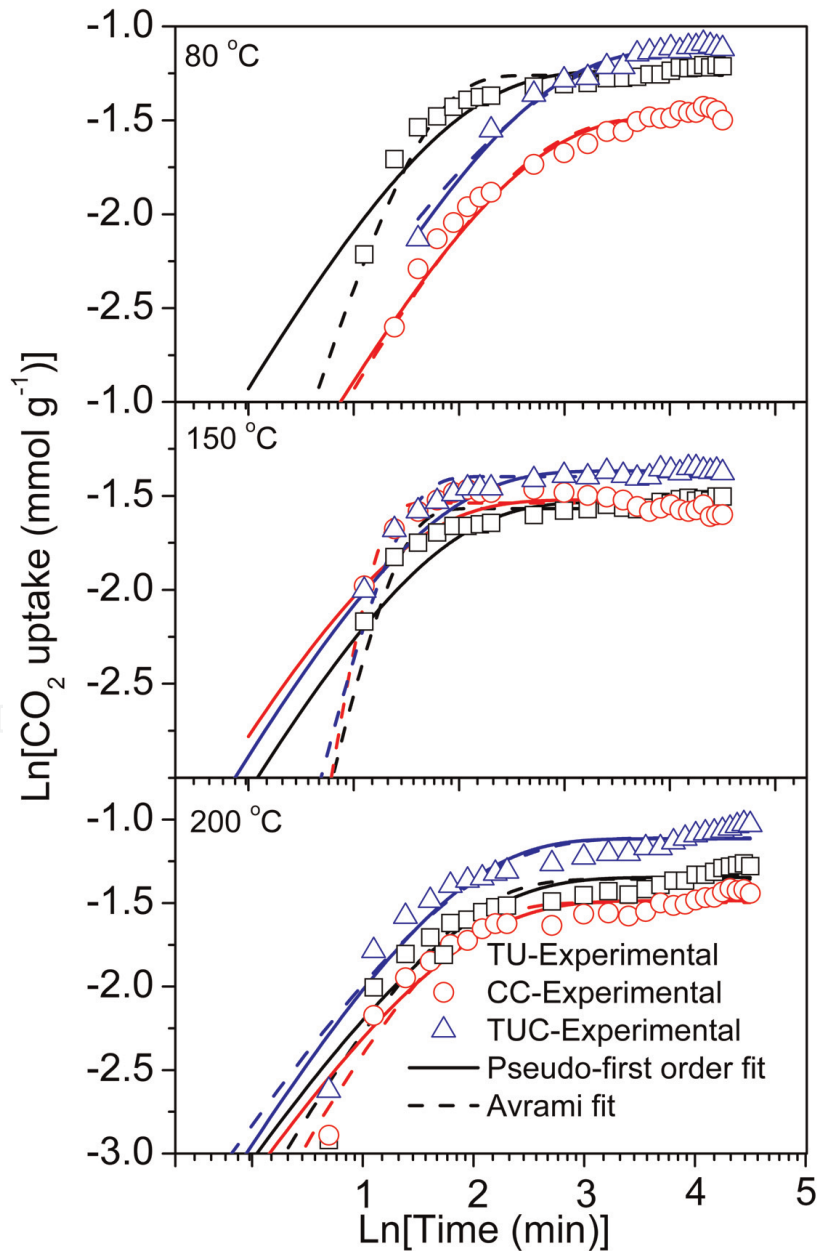


**Figure 7.**

Experimental CO<sub>2</sub> uptake on different LDHs at different temperatures and corresponding fit to kinetic models: (□) TU-LDHs, (○) CC-LDHs, (△) TUC-LDHs, (—) Pseudo-first order fit and (---) Avrami fit.

showed obvious two-stage adsorption process under different adsorption conditions. That means, adsorption process of CO<sub>2</sub> sorption by LDHs consists of a fast reaction stage and a much slower second stage controlled by CO<sub>2</sub> diffusion. Clearly, both of the models predict CO<sub>2</sub> adsorption process well. But, Avrami kinetic model offers a better description of the adsorption of CO<sub>2</sub>, since the R<sup>2</sup> value was higher and X<sup>2</sup> and Δq yielded low values in comparison of pseudo-first order model. Therefore, Avrami kinetic model is more suitable to predict the CO<sub>2</sub> adsorption process of LDHs in our experiment. **Table 3** shows the values of kinetic constants and the characteristic parameters from the kinetic model, along with the X<sup>2</sup>, Δq, R<sup>2</sup> as calculated using Eqs. (1)–(3). This is because pseudo-first order kinetic model is suitable for explaining the low surface coverage adsorption, and hence describes the early stages of adsorption [30, 31]. In the process of CO<sub>2</sub> adsorption by LDHs, it is not a simple physical adsorption process. LDHs consists of positively charged Mg-Al-OH brucite type network in an octahedral network. After calcination, the LDHs gradually loses its interlayer water and form a mixed oxide with sufficient basic sites which are favourable for CO<sub>2</sub> sorption. It is a complex reaction in combination of physical and chemical process during CO<sub>2</sub> uptake [19, 32]. Avrami kinetic model is logical to attribute the fitting of CO<sub>2</sub> uptake process in our experiment.

The pseudo-first order model and Avrami model kinetic parameters  $k_f$  and  $k_A$  are the time scales for measuring the process to reach equilibrium. The higher  $k_f$  and  $k_A$ , the quicker speed for the process to reach equilibrium. It can be observed from **Table 3** that  $k_f$  and  $k_A$  of CC-LDHs and TUC-LDHs increase with temperature overall. When the temperature increases, the molecule's speed (kinetic energy) also increases. So, the CO<sub>2</sub> molecules will migrate faster inside the pores, which in turn will result in an increase in the rate of diffusion. Hence, it is reflected in the form of CO<sub>2</sub> uptake curves with much steeper ones (shown in **Figure 7**). For TU-LDHs,  $k_f$  and  $k_A$  do not change much as the temperature increases. This might be caused by the fact that the pores of TU-LDHs are easy to saturate or block during the CO<sub>2</sub> adsorption even at high temperature due to its small pore size and volume. This phenomenon usually occurs in the microporous material such as porous MgO [33], zeolites [34] and active carbons [35]. The order of CO<sub>2</sub> adsorption capacity to reach equilibrium ( $k_A$ ) at 80°C seen in Avrami model is: TU-LDHs > TUC-LDHs > CC-LDHs. The order of CO<sub>2</sub> adsorption capacity to reach equilibrium at 150°C seen in Avrami model is: CC-LDHs > TU-LDHs = TUC-LDHs. When the CO<sub>2</sub> adsorption temperature is 200°C, the time of reaching equilibrium by three materials is almost the same. This indicates that TU-LDHs and TUC-LDHs show the potential application of reaching equilibrium to absorb the CO<sub>2</sub> gas at low temperature (<100°C). The Avrami exponent  $n_A$  reflects the extent of driving force on adsorption apparatus. The data of  $n_A$  in the range of 1–4 suggest that CO<sub>2</sub> adsorption occurs more than one-reaction pathway from adsorption sites [36].

Here, the schematic CO<sub>2</sub> adsorption mechanism on LDHs is shown in **Figure 8**. During the CO<sub>2</sub> adsorption process in porous material, it is known that CO<sub>2</sub> molecule diffuses through the gas film to pore structure among the agglomerate particles and the crystalline grains; or the CO<sub>2</sub> molecule interacts with the adsorbent (surface reaction). Generally, the surface reaction process is quite rapid, and the resistance associated with the surface adsorption can be assumed to be negligible [33]. The whole process of CO<sub>2</sub> adsorption can be simplified that CO<sub>2</sub> permeates in a tube with tubular structure. As mentioned above, TUC-LDHs has the largest BET surface area as well as pore size and volume. The effective absorbed area is larger and it is easy to absorb the CO<sub>2</sub> in the tubular tube with less resistance. This trend is obvious when the adsorption is operated at a high temperature. For the TU-LDHs, although it shows a second largest surface area, its pore size and volume are limited. The pores of LDHs are easy to block when the CO<sub>2</sub> concentration in the tubular tube

Parameters for Simulation												
Material	Temperature (°C)	Pseudo-first order model					Avrami model					
		$K_f$ (s <sup>-1</sup> )	$q_e$ (mmol g <sup>-1</sup> )	$X^2$	$\Delta q$ (%)	$R^2$	$K_f$ (s <sup>-1</sup> )	$q_e$ (mmol g <sup>-1</sup> )	$n_a$	$X^2$	$\Delta q$ (%)	$R^2$
TU-LDHs	80	0.20	0.29	0.021	7.05	0.9131	0.22	0.28	1.82	0.019	5.78	0.9544
	150	0.24	0.22	0.015	5.74	0.9149	0.27	0.21	2.64	0.019	6.68	0.9463
	200	0.20	0.26	0.024	6.93	0.9420	0.21	0.26	1.22	0.042	11.06	0.9434
CC-LDHs	80	0.10	0.23	0.017	11.18	0.9717	0.11	0.23	1.06	0.017	10.33	0.9708
	150	0.33	0.22	0.034	8.02	0.7791	0.32	0.21	3.9	0.013	5.14	0.9640
	200	0.21	0.23	0.16	21.42	0.9337	0.22	0.22	1.28	0.023	8.32	0.9399
TUC-LDHs	80	0.11	0.33	0.015	8.37	0.9774	0.12	0.32	1.1	0.016	7.35	0.9775
	150	0.25	0.25	0.013	5.04	0.9222	0.27	0.25	2.41	0.015	5.63	0.9727
	200	0.20	0.33	0.024	6.93	0.9447	0.20	0.33	1.09	0.043	11.06	0.9430

**Table 3.**  
*Values of the kinetic model parameters for CO<sub>2</sub> adsorption on LDHs.*

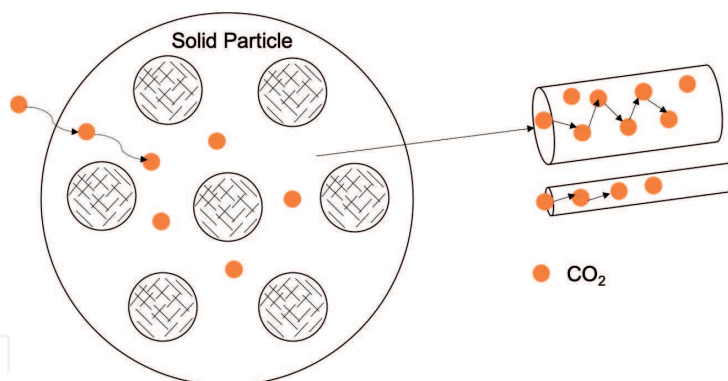


Figure 8.  
Schematic CO<sub>2</sub> adsorption mechanism on LDHs.

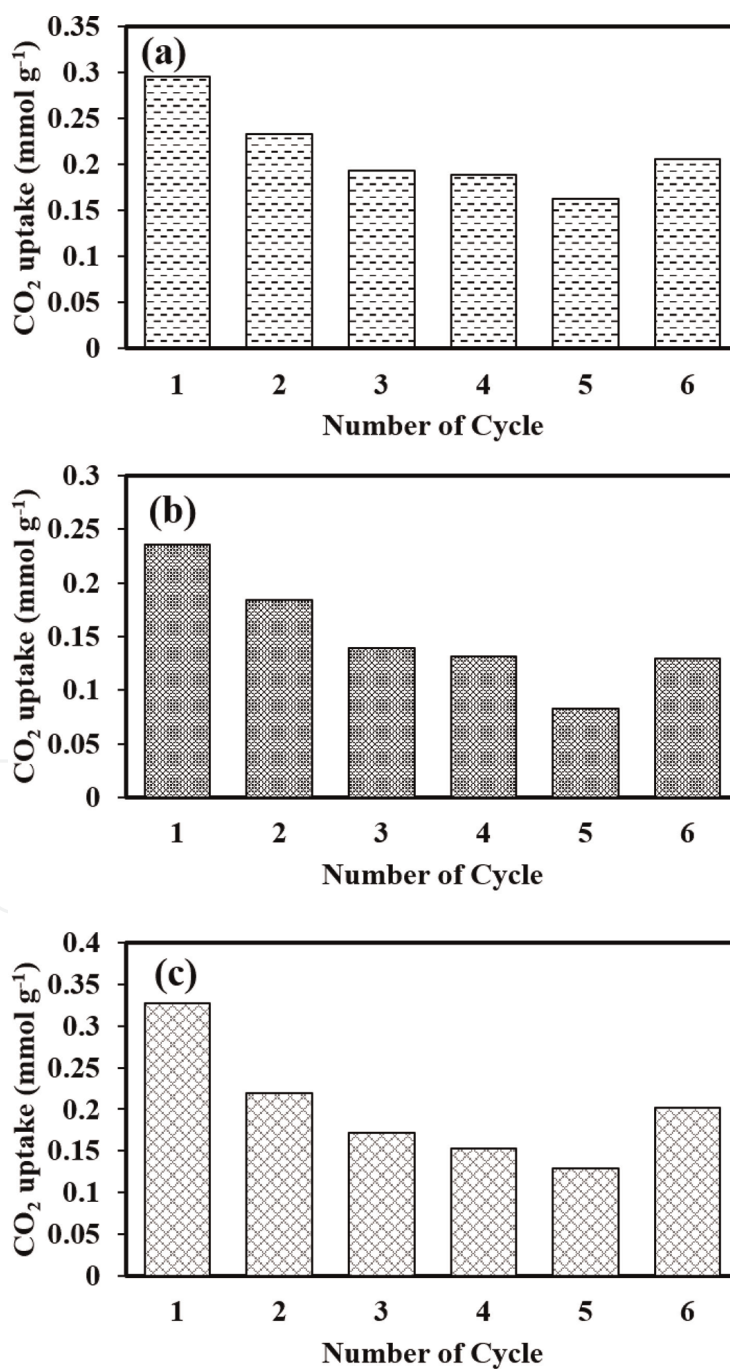


Figure 9.  
CO<sub>2</sub> uptake using temperature during six cycles at 80°C (a) TU-LDHs, (b) CC-LDHs and (c) TUC-LDHs.



increases; finally, the CO<sub>2</sub> diffusion rate will slow down. As for CC-LDHs, it has the lowest effective surface area, which finally influences its CO<sub>2</sub> adsorption ability.

### 3.5 CO<sub>2</sub> adsorption/desorption cycling test

For practical applications, the stability of adsorbents during the adsorption-desorption process should be considered. Hence, it is badly needed to test its cycle operation. **Figure 9** shows six successive runs of adsorption-desorption isotherms of LDHs at 80°C. TUC-LDHs shows an initial cyclic adsorption capacity (0.33 mmol g<sup>-1</sup>). However, it decreased to CO<sub>2</sub> adsorption capacity of 0.21 mmol g<sup>-1</sup> at second cycle, which is 67% of the original capacity. At six cycles of adsorption, the adsorption capacity is still 0.2 mmol g<sup>-1</sup> with 60.6% of the original capacity although CO<sub>2</sub> adsorption is fluctuated during the middle process. The decrease of adsorption capacity over several cycles has also been reported by several research groups. The main reason for the decrease of CO<sub>2</sub> adsorption is possible that some chemical sorption sites are blocked during the subsequent adsorption/desorption cycles. TU-LDHs and CC-LDHs show an initial CO<sub>2</sub> adsorption capacity of 0.30 and 0.24 mmol g<sup>-1</sup>, in which the retentions could achieve as high as 69.8 and 54.7%, respectively. These results indicate that the TU process played a role not only in increasing CO<sub>2</sub> sorption capacity, but also in improving the cyclic performance. The experimental results show that stability of hydrotalcites synthesized by both TUC and TU method are higher than the conventional prepared LDHs, which seems promising adsorbents for CO<sub>2</sub> adsorption.

## 4. Conclusions

The present studies have demonstrated that the MgAl LDHs as a CO<sub>2</sub> adsorbent can be synthesized successfully through an ultrasonic assisted ‘T-mixer’ (TU-LDHs), hybrid two-step preparation method (TUC-LDHs) and conventional co-preparation (CC-LDHs) method. The conclusions reached as the results of the current study are as follows:

1. It was found that the prepared TUC-LDHs had a clear layered structure and the average size was approximately 100 nm with the largest surface area, which makes it a promising adsorbent material for CO<sub>2</sub> capture in practical application.
2. Increasing the adsorption temperature is benefit to improve the CO<sub>2</sub> adsorption capacity of LDHs. The highest capture capacity was got when the CO<sub>2</sub> adsorption took place at 200°C by TUC-LDHs.
3. The CO<sub>2</sub> adsorption stability of TU-LDHs and TUC-LDHs is higher than the CC-LDHs after six adsorption/desorption cycles.

## Acknowledgements

This work was financially supported by National Natural Science Foundation of China (NSFC) (Grant No. 21576141) and Zhejiang Provincial Natural Science Foundation (Grant No. LY15B060001). This work was carried out at the International Doctoral Innovation Centre (IDIC). Xiani Huang would also like to

acknowledge the support through the Ph.D. scholarship of the International Doctoral Innovation Centre (IDIC) of University of Nottingham Ningbo China.

## Abbreviations

TU-LDHs	MgAl LDHs prepared by ultrasonication-intensified in ‘T-mixer’
CC-LDHs	MgAl LDHs prepared by conventional co-precipitation
TUC-LDHs	MgAl LDHs prepared by ultrasonic-intensified in ‘T-mixer’ pretreatment followed by conventional co-precipitation

## Author details


Xiani Huang<sup>1</sup>, Xiaogang Yang<sup>1\*</sup>, Guang Li<sup>1</sup>, Collins I. Ezeh<sup>1</sup>, Chenggong Sun<sup>2</sup> and Collins Snape<sup>2</sup>

<sup>1</sup> Department of Mechanical, Materials and Manufacturing Engineering, University of Nottingham Ningbo China, Ningbo, P.R. China

<sup>2</sup> Department of Chemical and Environmental Engineering, University of Nottingham, University Park, Nottingham, UK

\*Address all correspondence to: [xiaogang.yang@nottingham.edu.cn](mailto:xiaogang.yang@nottingham.edu.cn)

## IntechOpen

© 2019 The Author(s). Licensee IntechOpen. This chapter is distributed under the terms of the Creative Commons Attribution License (<http://creativecommons.org/licenses/by/3.0>), which permits unrestricted use, distribution, and reproduction in any medium, provided the original work is properly cited. 

## References

- [1] Yu C-H, Huang C-H, Tan C-S. Mint: A review of CO<sub>2</sub> capture by absorption and adsorption. *Aerosol and Air Quality Research*. 2012;**12**:745-769. DOI: 10.4209/aaqr.2012.05.0132
- [2] Stevens L, Williams K, Han WY, Drage T, Snape C, Wood J, et al. Mint: Preparation and CO<sub>2</sub> adsorption of diamine modified montmorillonite via exfoliation grafting route. *Chemical Engineering Journal*. 2013;**215–216**: 699-708. DOI: 10.1016/j.cej.2012.11.058
- [3] Manohara GV. Mint: Exfoliation of layered double hydroxides (LDHs): A new route to mineralize atmospheric CO<sub>2</sub>. *RSC Advances*. 2014;**4**: 46126-46132. DOI: 10.1039/C4RA08865D
- [4] Kou X, Guo H, Ayele EG, Li S, Zhao Y, Wang S, et al. Mint: Adsorption of CO<sub>2</sub> on MgAl-CO<sub>3</sub> LDHs-derived sorbents with 3D nanoflower-like structure. *Energy and Fuels*. 2018;**32**: 5313-5320. DOI: 10.1021/acs.energyfuels.8b00024
- [5] Wang J, Stevens LA, Drage TC, Wood J. Mint: Preparation and CO<sub>2</sub> adsorption of amine modified Mg–Al LDH via exfoliation route. *Chemical Engineering Science*. 2012;**68**:424-431. DOI: 10.1016/j.ces.2011.09.052
- [6] Yong Z, Rodrigues AE. Mint: Adsorption of carbon dioxide onto hydrotalcite-like compounds (HTLcs) at high temperatures. *Industrial and Engineering Chemistry Research*. 2001;**40**:204-209. DOI: 10.1021/ie000238w
- [7] Aschenbrenner O, McGuire P, Alsamaq S, Wang J, Supasitmongkol S, Al-Duri B, et al. Mint: Adsorption of carbon dioxide on hydrotalcite-like compounds of different compositions. *Chemical Engineering Research and Design*. 2011;**89**:1711-1721. DOI: 10.1016/j.cherd.2010.09.019
- [8] Wang Q, Tay HH, Ng DJW, Chen L, Liu Y, Chang J, et al. Mint: The effect of trivalent cations on the performance of Mg-M-CO<sub>3</sub> layered double hydroxides for high-temperature CO<sub>2</sub> capture. *ChemSusChem*. 2010;**3**:965-973. DOI: 10.1002/cssc.201000099
- [9] Hutson ND, Attwood BC. Mint: High temperature adsorption of CO<sub>2</sub> on various hydrotalcite-like compounds. *Adsorption*. 2008;**14**:781-789. DOI: 10.1007/s10450-007-9085-6
- [10] Hou XJ, Li H, He P, Sun Z, Li S. Mint: Structural and electronic analysis of Li/Al layered double hydroxides and their adsorption for CO<sub>2</sub>. *Applied Surface Science*. 2017;**416**:411-423. DOI: 10.1016/j.apsusc.2017.04.187
- [11] Kim S, Jeon SG, Lee KB. Mint: High-temperature CO<sub>2</sub> sorption on hydrotalcite having a high Mg/Al molar ratio. *ACS Applied Materials and Interfaces*. 2016;**8**:5763-5767. DOI: 10.1021/acsami.5b12598
- [12] Gao Y, Zhang Z, Wu J, Yi X, Zheng A, Umar A, et al. Mint: Comprehensive investigation of CO<sub>2</sub> adsorption on Mg-Al-CO<sub>3</sub> LDH-derived mixed metal oxides. *Journal of Materials Chemistry A*. 2013;**1**:12782-12790. DOI: 10.1039/c3ta13039h
- [13] Silva JM, Trujillano R, Rives V, Soria MA, Madeira LM. Mint: High temperature CO<sub>2</sub> sorption over modified hydrotalcites. *Chemical Engineering Journal*. 2017;**325**:25-34. DOI: 10.1016/j.cej.2017.05.032
- [14] Oliveira ELG, Grande CA, Rodrigues AE. Mint: CO<sub>2</sub> sorption on hydrotalcite and alkali-modified (K and Cs) hydrotalcites at high temperatures. *Separation and Purification Technology*. 2008;**62**:137-147. DOI: 10.1016/j.seppur.2008.01.011

- [15] Zhu X, Chen C, Wang Q, Shi Y, O'Hare D, Cai N. Mint: Roles for K<sub>2</sub>CO<sub>3</sub> doping on elevated temperature CO<sub>2</sub> adsorption of potassium promoted layered double oxides. *Chemical Engineering Journal*. 2019;**366**:181-191. DOI: 10.1016/j.cej.2019.01.192
- [16] Kim S, Lee KB. Mint: Impregnation of hydrotalcite with NaNO<sub>3</sub> for enhanced high-temperature CO<sub>2</sub> sorption uptake. *Chemical Engineering Journal*. 2019;**356**:964-972. DOI: 10.1016/j.cej.2018.08.207
- [17] Hanif A, Dasgupta S, Divekar S, Arya A, Garg MO, Nanoti A. Mint: A study on high temperature CO<sub>2</sub> capture by improved hydrotalcite sorbents. *Chemical Engineering Journal*. 2014;**236**:91-99. DOI: 10.1016/j.cej.2013.09.076
- [18] Ram Reddy MK, Xu ZP, Lu GQM, Diniz da Costa JC. Mint: Influence of water on high-temperature CO<sub>2</sub> capture using layered double hydroxide derivatives. *Industrial and Engineering Chemistry Research*. 2008;**47**: 2630-2635. DOI: 10.1021/ie0716060
- [19] Ram Reddy MK, Xu ZP, (Max) Lu GQ, Diniz da Costa JC. Mint: Layered double hydroxides for CO<sub>2</sub> capture: Structure evolution and regeneration. *Industrial & Engineering Chemistry Research*. 2006;**45**:7504-7509. DOI: 10.1021/ie060757k
- [20] Wang Q, Gao Y, Luo J, Zhong Z, Borgna A, Guo Z, et al. Mint: Synthesis of nano-sized spherical Mg<sub>3</sub>Al-CO<sub>3</sub> layered double hydroxide as a high-temperature CO<sub>2</sub> adsorbent. *RSC Advances*. 2013;**3**:3414-3420. DOI: 10.1039/c2ra22607c
- [21] Ramírez-Moreno MJ, Romero-Ibarra IC, Hernández-Pérez MA, Pfeiffer H. Mint: CO<sub>2</sub> adsorption at elevated pressure and temperature on Mg-Al layered double hydroxide. *Industrial and Engineering Chemistry Research*. 2014;**53**:8087-8094. DOI: 10.1021/ie5010515
- [22] Martunus OMR, Fernando WJN. Mint: Elevated temperature carbon dioxide capture via reinforced metal hydrotalcite. *Microporous and Mesoporous Materials*. 2011;**138**: 110-117. DOI: 10.1016/j.micromeso.2010.09.023
- [23] Dong B, Huang X, Yang X, Li G, Xia L, Chen G. Mint: Rapid preparation of high electrochemical performance LiFePO<sub>4</sub>/C composite cathode material with an ultrasonic-intensified micro-impinging jetting reactor. *Ultrasonics Sonochemistry*. 2017;**39**:816-826. DOI: 10.1016/j.ultsonch.2017.06.010
- [24] Dong B, Li G, Yang X, Chen L, Chen GZ. Mint: Controllable synthesis of (NH<sub>4</sub>)Fe<sub>2</sub>(PO<sub>4</sub>)<sub>2</sub>(OH)<sub>2</sub>H<sub>2</sub>O using two-step route: Ultrasonic-intensified impinging stream pre-treatment followed by hydrothermal treatment. *Ultrasonics Sonochemistry*. 2018;**42**: 452-463. DOI: 10.1016/j.ultsonch.2017.12.008
- [25] Mallakpour S, Dinari M, Behranvand V. Mint: Ultrasonic-assisted synthesis and characterization of layered double hydroxides intercalated with bioactive N,N'-(pyromellitoyl)-bis- $\alpha$ -amino acids. *RSC Advances*. 2013;**3**:23303-23308. DOI: 10.1039/c3ra43645d
- [26] Sing KSW, Everett DH, Haul RAW, Moscou L, Pierotti RA, Rouquerol J, et al. Mint: Reporting physisorption data for gas solid systems with special reference to the determination of surface area and porosity. *Pure and Applied Chemistry*. 1985;**57**:603-619. DOI: 10.1351/pac198557040603
- [27] Carrado KA, Csencsits R, Thiyagarajan P, Seifert S, Macha SM, Harwood J. Mint: Crystallization and textural porosity of synthetic clay minerals. *Journal of Materials*

- Chemistry. 2002;**12**:3228-3237. DOI: 10.1039/b204180b
- [28] Gunjakar JL, Kim IY, Lee JM, Lee N-S, Hwang S-J. Mint: Self-assembly of layered double hydroxide 2D nanoplates with graphene nanosheets: An effective way to improve the photocatalytic activity of 2D nanostructured materials for visible light-induced O<sub>2</sub> generation. *Energy and Environmental Science*. 2013;**6**:1008-1017. DOI: 10.1039/C3EE23989F
- [29] Wang J, Huang L, Zheng Q, Qiao Y, Wang Q. Mint: Layered double hydroxides/oxidized carbon nanotube nanocomposites for CO<sub>2</sub> capture. *Journal of Industrial and Engineering Chemistry*. 2016;**36**:255-262. DOI: 10.1016/j.jiec.2016.02.010
- [30] Serna-Guerrero R, Sayari A. Mint: Modeling adsorption of CO<sub>2</sub> on amine-functionalized mesoporous silica. 2: kinetics and breakthrough curves. *Chemical Engineering Journal*. 2010;**161**:182-190. DOI: 10.1016/j.cej.2010.04.042
- [31] Loganathan S, Tikmani M, Edubilli S, Mishra A, Ghoshal AK. Mint: CO<sub>2</sub> adsorption kinetics on mesoporous silica under wide range of pressure and temperature. *Chemical Engineering Journal*. 2014;**256**:1-8. DOI: 10.1016/j.cej.2014.06.091
- [32] Wang J, Mei X, Huang L, Zheng Q, Qiao Y, Zang K, et al. Mint: Synthesis of layered double hydroxides/graphene oxide nanocomposite as a novel high-temperature CO<sub>2</sub> adsorbent. *Journal of Energy Chemistry*. 2015;**24**:127-137. DOI: 10.1016/s2095-4956(15)60293-5
- [33] Song G, Zhu X, Chen R, Liao Q, Ding Y-D, Chen L. Mint: An investigation of CO<sub>2</sub> adsorption kinetics on porous magnesium oxide. *Chemical Engineering Journal*. 2016;**283**:175-183. DOI: 10.1016/j.cej.2015.07.055
- [34] Li P, Tezel H. Mint: Equilibrium and kinetic analysis of CO<sub>2</sub>-N<sub>2</sub> adsorption separation by concentration pulse chromatography. *Journal of Colloid and Interface Science*. 2007;**313**:12-17. DOI: 10.1016/j.jcis.2007.04.015
- [35] Saha D, Deng S. Mint: Adsorption equilibrium and kinetics of CO<sub>2</sub>, CH<sub>4</sub>, N<sub>2</sub>O, and NH<sub>3</sub> on ordered mesoporous carbon. *Journal of Colloid and Interface Science*. 2010;**345**:402-409. DOI: 10.1016/j.jcis.2010.01.076
- [36] Liu Q, Shi J, Zheng S, Tao M, He Y, Shi Y. Mint: Kinetics studies of CO<sub>2</sub> adsorption/desorption on amine-functionalized multiwalled carbon nanotubes. *Industrial and Engineering Chemistry Research*. 2014;**53**: 11677-11683. DOI: 10.1021/ie502009n